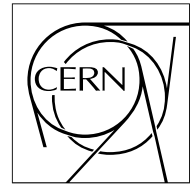


The Compact Muon Solenoid Experiment

CMS Note

Mailing address: CMS CERN, CH-1211 GENEVA 23, Switzerland



December, 1999

Evaluation and selection of analogue optical links for the CMS tracker - methodology and application

F. Jensen, C.S Azevedo, L. Björkman, G.Cervelli, K.Gill, R.Grabit, F.Vasey

CERN, Geneva, Switzerland

Abstract

A methodology for analysing the analogue performance of the optical link for the CMS tracker has been developed. The methodology enables, through a process of data compaction, easy comparison between different link alternatives. It is demonstrated how the best link configurations can be found in terms of system performance. The described method is also a first step towards a procedure to track performance during the link production and installation phase.

1 Introduction

Optical links are being developed for the CMS tracker. Over 50000, 100m long, analog links are required to read out tracking data [1-3]. Prototype optical links have now been successfully developed that satisfy the stringent requirements for system performance [4], radiation hardness [5] and reliability [6], and the final component selection procedure has been initiated.

In light of the large number of links to be installed in the tracker it is advantageous, for cost reasons, to use commercial-of-the-shelf (COTS) components. The use of COTS also has the advantage of reducing system development time. However COTS components are not validated for the environment to be encountered in the CMS tracker, thus it is necessary to carefully evaluate all components for environmental resistance [5,6]. In addition COTS optoelectronic components are typically only tested by the manufacturer for digital applications, therefore the *analogue performance* of the link components has to be evaluated. For this purpose a reliable and stable experimental setup for measuring the analogue link performance has been developed [7].

This paper will discuss the methodology that has been developed for analyzing the analogue performance of candidate optical read-out links for the CMS tracker. It will be shown how the analogue performance is quantified and compacted by averaging over parts of the input range, as well as over groups of links, to arrive at a figure-of-merit plot for signal-to-noise ratio and nonlinearity. The method will also facilitate qualification during pre-production and installation of the links.

In the first part of the paper the performance evaluation methodology is explained in detail. In the second part the developed method is applied to an example set of measured link data. Measured performance data from four groups of links will be analyzed for a total of 80 links. It will be shown how each of the links tested fit within the specification limits set on the CMS tracker links. Moreover it will be demonstrated how a comparison between the different link alternatives can be made, and typical system performance will be extracted.

2 Performance evaluation - methodology

The optical link system under consideration in this paper consists of laser driver, 1310nm semiconductor laser transmitter, single-mode optical fiber with 1 to 3 breakpoints, p-i-n photodiode and transimpedance receiver. Further details on the experimental method and optical link system are given in section 3.1.

The evaluation of the optical links is based on the measurement of the system static transfer characteristic and is described in the following section.

2.1 Analogue performance measures

The measured parameters include system input, X , output voltage, $Y(X)$, and RMS-noise $dY(X)$. These parameters are processed to give information on linearity and dynamic range. About 100 static voltage levels, X , are fed sequentially to the system input as a ramp. For each static measurement point the average, $Y(X)$, and standard deviation, $dY(X)$, of the link output voltage is measured. A typical link transfer characteristic is shown in Fig. 1. The full input range, X , is 0.8V, with the working point set to be at 0V. The full operating input range, ΔX , that will be considered is thus 0.0-0.8V. Shown in Fig. 1 is also a typical 0.25V input pulse, which gives an output pulse of 0.53V with the given gain of 2.1V/V. The curved region at about -0.2V input voltage corresponds to the laser threshold.

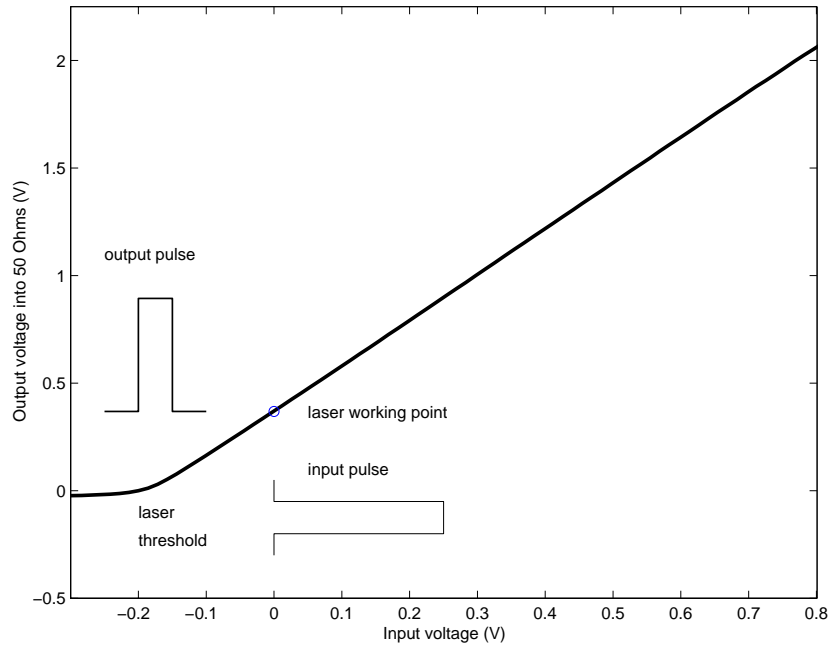


Fig. 1: Typical link transfer characteristic measured into 50Ω .

In the following the analysis of X , $Y(X)$ and $dY(X)$ will be explained using a "typical" data set of 20 links. These links are typical in the sense that the final CMS link is expected to have a performance close to the data shown, and the bulk of the links tested so far have an analogue performance close to the 20 links shown. Upper specification limits (USL) will be introduced in the performance plots to show the usefulness of the methodology, however the levels chosen are tentative at this stage and should not be understood as the final specification limits.

2.1.1 Static transfer characteristic

In Fig. 2 the transfer characteristics for a typical set of 20 optical links are shown. The link gains, G , are estimated from a linear regression fit over a range extending from the working point ($X=0V$) up to $X=0.4V$. The operating range considered is as stated in the previous paragraph between $0.0V$ (thick vertical line) and $0.8V$. The laser thresholds have all been aligned to $-0.2V$ input voltage to ease comparison between links.

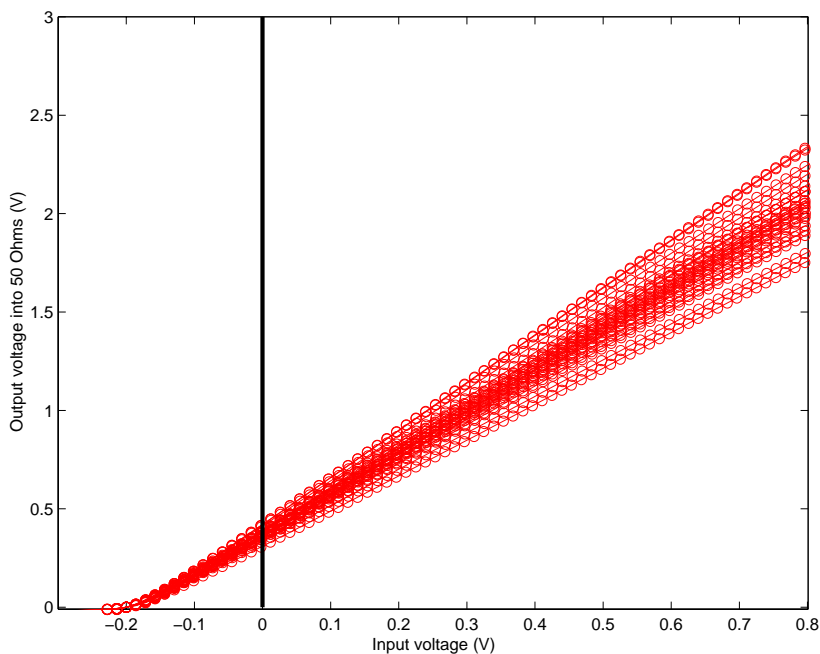


Fig. 3: Measured typical transfer characteristics for 20 optical channels.

2.1.2 Normalised RMS-noise

The system gain for an optical link depends on a number of factors, both electrical and optical, including the number of optical connections in the optical path and quality of those connections. Therefore, in order to have a gain-independent measure of noise, the measured RMS-noise, $dY(X)$, is normalised with the estimated gain, G , for a fixed normalisation voltage, ΔX . The normalised RMS-noise, $dY_{norm}(X)$, is then given in percent by:

$$dY_{norm}(X) = \frac{dY(X)}{G\Delta X} \times 100 \quad (2-1)$$

It is also useful to introduce the *peak-signal* to noise ratio, $PSNR$, as

$$PSNR = \frac{G\Delta X}{dY(X)} = \frac{100}{dY_{norm}(X)} \quad (2-2)$$

An upper limit on the normalised noise can be defined using the minimum signal-to-noise ratio, SNR , given as 256:1 at peak input signal, $X_{peak}=0.8V$ ¹:

$$SNR(X) = \frac{Y(X)}{dY(X)} \geq 320X, \quad (2-3)$$

and therefore

$$dY_{norm}(X) = \frac{100}{SNR(X)} \times \frac{Y(X)}{G\Delta X} \approx \frac{100}{SNR(X)} \times \frac{GX}{G\Delta X} \leq \frac{100}{320X} \times \frac{X}{\Delta X} = \frac{0.3125}{\Delta X} = \text{USL} \quad (2-4)$$

Here the upper specification limit, USL, on the normalised noise has been introduced. For a normalisation voltage $\Delta X=0.8V$ this gives an USL of 0.391% normalised RMS-noise. The normalised RMS-noise, $dY_{norm}(X)$, is shown in Fig. 3 for an input range of 0.8V for the typical set of 20 links.

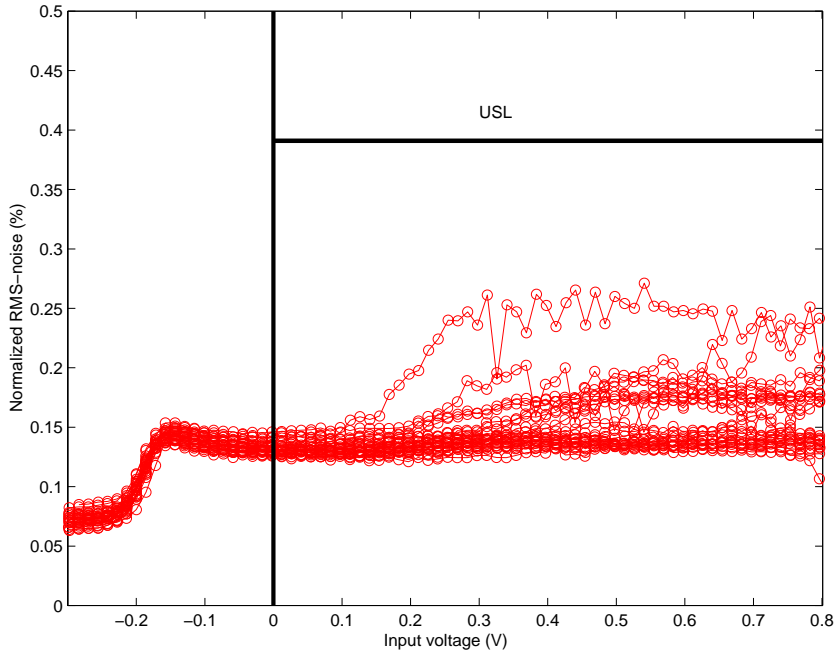


Fig. 3: Normalised RMS-noise for 20 optical channels. Maximum allowed normalised RMS-noise, $dY_{norm}=0.391\%$, is shown as a full horizontal line marked USL (Upper Specification Limit). Scale on y-axis is in percent of full scale, $G\Delta X$, with $\Delta X=0.8V$.

¹ In the draft link specification (Ref. [8]) the minimum link signal-to-noise ratio is given as 48dB for peak input signal. The 0.8V peak input signal corresponds to the linear range of the laser driver.

2.1.3 Integral nonlinearity

The measure used to quantify deviation from linearity is integral nonlinearity, $INL(X)$, defined in percent as:

$$INL(X) = \frac{|Y(X) - GX|}{G\Delta X} \times 100 \quad (2-5)$$

It should be kept in mind that the position in X and width of the range chosen for the regression line fit (to extract the gain, G) influences the final calculated nonlinearity to some extent. A fitting range of 0.0-0.4V has been found to be a reasonable compromise that results in good linearity at both small and larger input signals.

Another useful definition of nonlinearity is relative deviation from linearity, RDL , defined in [7] as

$$RDL(X) = \frac{|Y(X) - GX|}{GX} \times 100 \quad (2-6)$$

Here the normalisation factor is the estimated output signal, as opposed to the full output signal. Relative deviation from linearity is useful, in particular for the system user, as it gives direct information on the amount of nonlinearity added by the optical link to a readout chain. However RDL in general diverges around the working point as $X \rightarrow 0V$. To avoid this problem it is convenient to have USL expressed in terms of integral nonlinearity, and approximate a single, fixed relative deviation from linearity, with a multi-range upper bound on INL . An upper bound on RDL can be transformed into an USL on the integral nonlinearity as

$$INL(X) = RDL(X) \times \frac{X}{\Delta X} \leq RDL_{USL} \times \frac{X}{\Delta X} \quad (2-7)$$

The upper specification limit on INL will thus be given by a straight line with slope $RDL_{USL}/\Delta X$. The integral nonlinearity for the typical set is displayed in Fig. 4 for $\Delta X=0.8V$. Arbitrarily specifying $RDL_{USL}=2.67\%$ the resulting upper specification limit on INL is the full sloping line in Fig. 7 (marked USL). The analysis is simplified (see also later sections for justification) by dividing the input range into four sub-ranges of interest: 0-1/8, 1/8-1/4, 1/4-1/2 and 1/2-1/1 of the full range of 0.8V, with corresponding limits on INL for each range. With a limit of $RDL_{USL}=2.67\%$ the resulting average INL_{USL} are shown in Fig. 7 for each of the four ranges. In Section 2.2.4 it will be shown how this subdivision facilitates easy comparison between links.

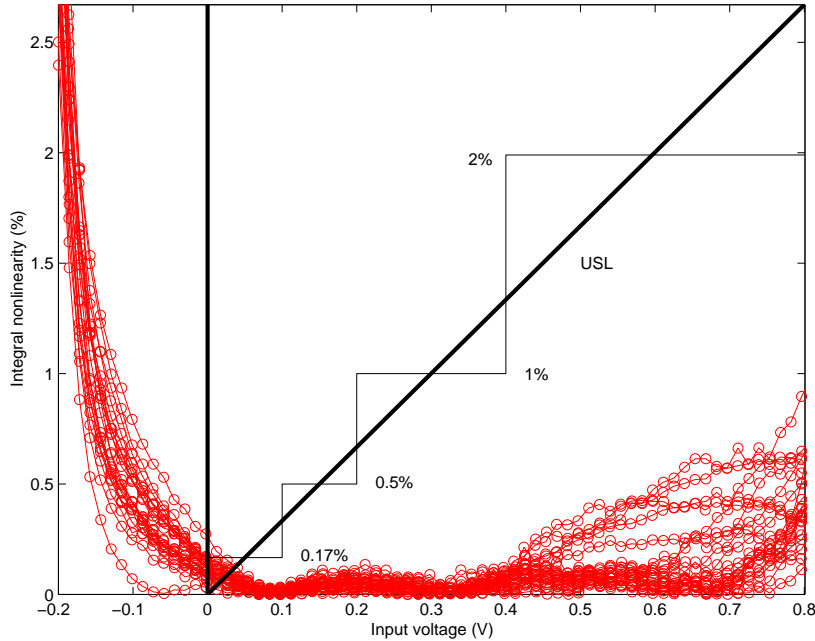


Fig 4: Integral nonlinearity for 20 optical channels. Scale on y-axis is in percent of full scale, $G\Delta X$, with $\Delta X=0.8V$.

2.2 Data reduction - averaging of analogue performance parameters

As larger quantities of optical channels are tested it becomes possible to extract typical system behaviour and parameter spread, as well as making forecasts on the performance of the full system of 50000 readout links. These forecasts will be of use both to the system designer and the system user to track the performance of the optical links during the production phase. Another benefit of testing large number of channels is that it becomes possible to compare and select with confidence components optimal with respect to system performance. Unfortunately, as the number of measured channels increases, the legibility of the plots shown decreases. From examining the data in Fig. 4 and 5, it becomes clear that already at a relatively low number of measurements it becomes unwieldy to visualise the full data set for performance evaluation and comparison.

A first step towards the goal of extracting typical system performance is taken by averaging measured performance data over groups of links. How this is done will be shown in Sections 2.2.1 to 2.2.3. In Section 2.2.4 it will then be demonstrated how performance "figures-of-merit" can be calculated that facilitate easy comparison between different link alternatives. These procedures also form the first step towards a full qualification procedure during link production and installation².

2.2.1 Average link transfer characteristic

For the link transfer characteristic, $Y(X)$, the average for a group of links is

$$\overline{Y(X)} = \frac{1}{N} \sum_{i=1}^N Y_i(X), \quad (2-8)$$

with the corresponding sample standard deviation

$$\sigma_Y(X) = \sqrt{\frac{1}{N-1} \sum_{i=1}^N (Y_i(X) - \overline{Y(X)})^2}, \quad (2-9)$$

where N is the number of links in each group. In Fig. 5 the average and standard deviation of the transfer characteristics for the 20 tested typical links are shown.

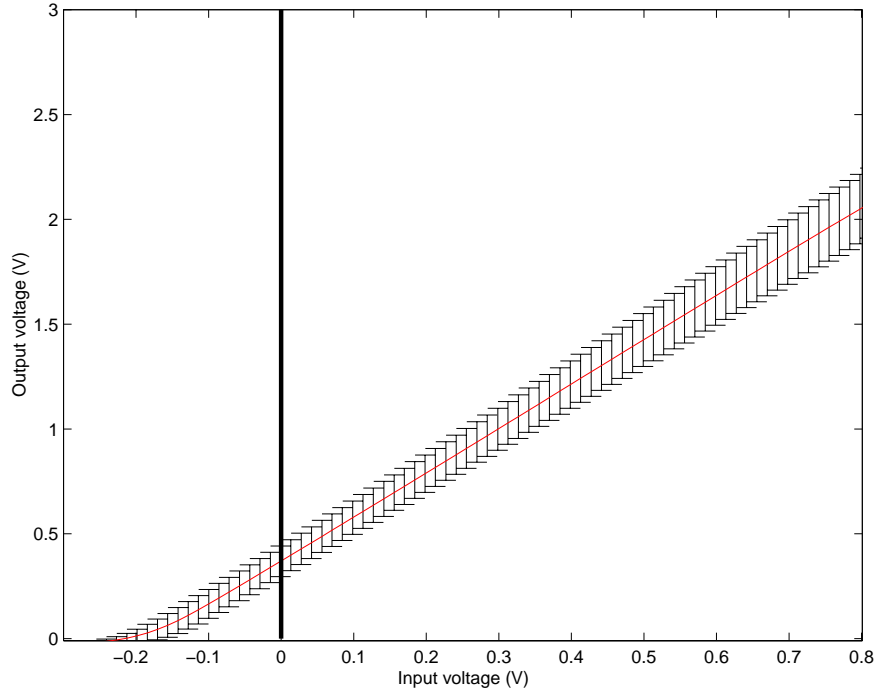


Fig. 5: Average and standard deviation of transfer characteristic of 20 optical channels.

² The complete quality control and process analysis procedure to be used for tracking link performance during the production phase will be the subject of a future CMS note.

2.2.2 Average normalised RMS-noise

The average of the normalised RMS-noise over a group of links is³:

$$\overline{dY(X)} = \frac{1}{N} \sum_{i=1}^N dY_i(X), \quad (2-10)$$

with corresponding standard deviation

$$\sigma_{dY(X)} = \sqrt{\frac{1}{N-1} \sum_{i=1}^N (dY_i(X) - \overline{dY(X)})^2} \quad (2-11)$$

The measured average normalised RMS-noise is shown in Fig. 6.

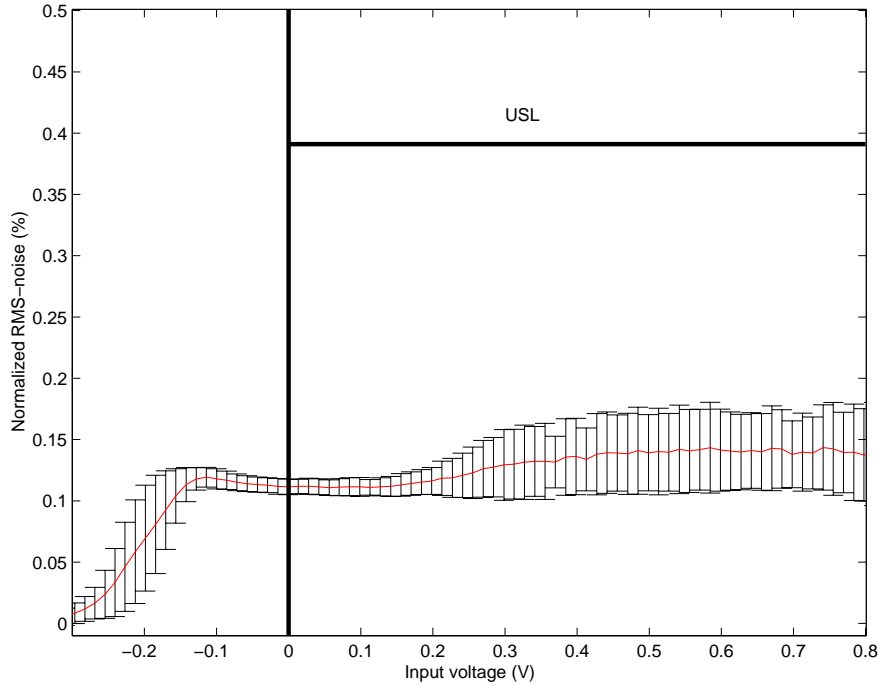


Fig. 6: Average and standard deviation of normalised RMS-noise of 20 optical channels. Scale on y-axis is in percent of full scale, $G\Delta X$, with $\Delta X=0.8V$.

2.2.3 Average integral nonlinearity

The average of the link integral nonlinearity over a group of links is

$$\overline{INL(X)} = \frac{1}{N} \sum_{i=1}^N INL_i(X), \quad (2-12)$$

with corresponding standard deviation

$$\sigma_{INL(X)} = \sqrt{\frac{1}{N-1} \sum_{i=1}^N (INL_i(X) - \overline{INL(X)})^2} \quad (2-13)$$

The calculated average of the integral nonlinearity, INL , is shown in Fig. 7 for 20 typical optical channels.

³ The subscript *norm* is dropped to simplify the notation here and in the following unless otherwise noted.

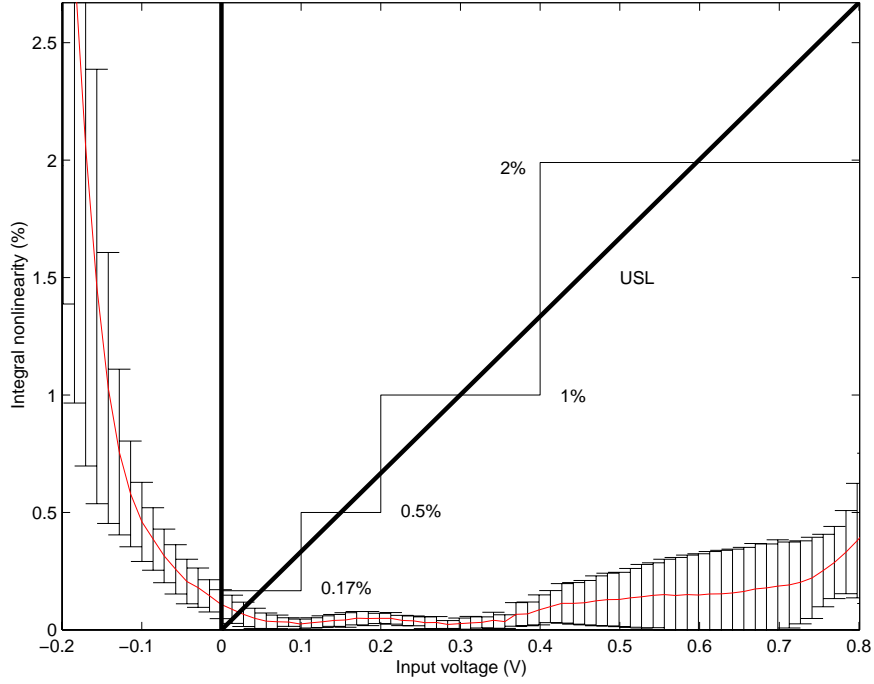


Fig. 7: Average and standard deviation of integral nonlinearity of 20 optical channels. Scale on y-axis is in percent of full-scale (0.8V). Scale on y-axis is in percent of full scale, $G\Delta X$, with $\Delta X=0.8V$.

2.2.4 Figure of merit for noise and linearity - averaging over input ranges

The final aim of the compaction of the measured data is to have one point per measured link, or possibly even per group of links, in each of the four input ranges considered. To achieve this the data is divided into ranges as explained in section 2.1.3, corresponding to 0-1/8, 1/8-1/4, 1/4-1/2 and 1/2-1/1 of the full input voltage range of 0.8V. This is done for the integral nonlinearity as well as for the normalised noise or equivalently, peak-signal to noise ratio. The figures of merit used for link comparisons are then defined to be the average of the peak-signal to noise ratio, $PSNR$, and the integral nonlinearity, INL , over the four ranges. The average $PSNR$ will be

$$\overline{PSNR}_{ik} = \frac{1}{X_{k+1} - X_k} \int_{X_k}^{X_{k+1}} PSNR_{ik}(S) dS, \quad (2-14)$$

where the subscript $norm$ has been dropped and the noise is normalised as

$$PSNR_{ik}(X) = \frac{G(X_{k+1} - X_0)}{dY_i(X)} \quad (2-15)$$

The index, $i=1, 2, \dots, N$, gives the link (or measurement) number and the index $k=0, 1, 2, 3$ gives the input range of interest: $X_{k+1}-X_k=0.1, 0.1, 0.4$ and $0.8V$ for $k=0, 1, 2, 3$.

The corresponding standard deviation is

$$\sigma_{PSNR_{ik}} = \sqrt{\frac{1}{X_{k+1} - X_k} \int_{X_k}^{X_{k+1}} PSNR_{ik}^2(S) dS - (\overline{PSNR}_{ik})^2} \quad (2-16)$$

A similar analysis is carried out for INL to give the average INL over the four ranges.

Carrying out the average over the input ranges for INL and $PSNR$ the result for the range 1/2-1/1 of the full input range ($k=3$) are displayed in a "figure of merit" plot as shown in Fig. 8. Each measured link is marked with a symbol for both mean INL and $PSNR$ with corresponding standard deviations. In Fig. 8 the limits shown are the limit on the peak-signal to noise ratio 256:1 for $k=3$ and the 2% average limit on integral nonlinearity.

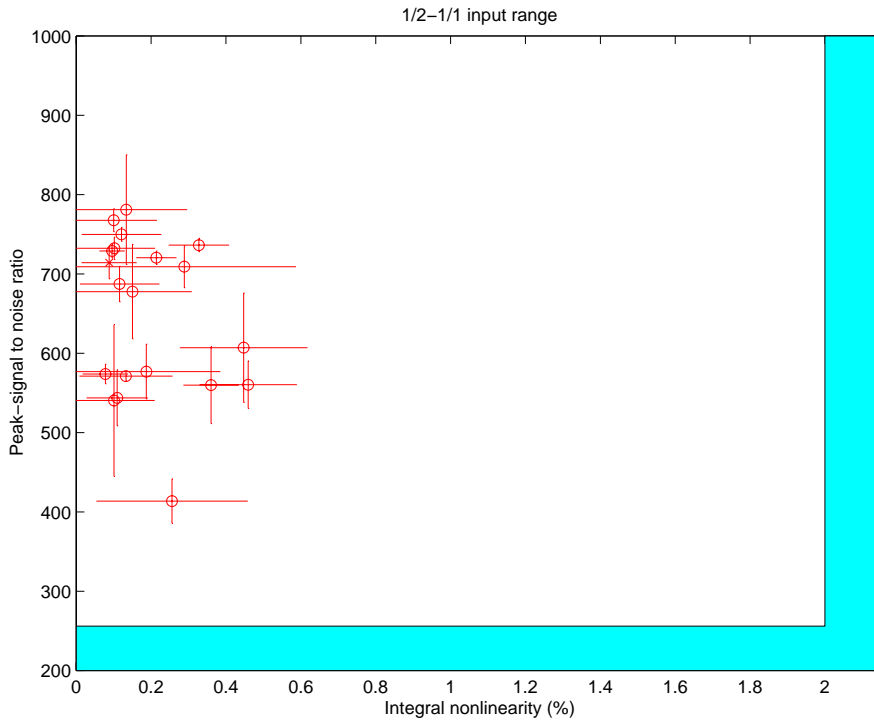


Fig. 8: Figure of merit plot for integral nonlinearity vs. peak-signal to noise ratio for 20 optical channels over the range 1/2-1/1 of the full input signal of 0.8V. Specification limits shown correspond to a signal to noise ratio of 256:1 and an integral nonlinearity of 2%.

Table 1 gives all the specification limits on noise and deviation from linearity. The USL used in the figure-of-merit plots are marked in grey. Note that the acceptance limits given are tentative at this stage.

Table 1: Upper specification limits

fraction of full range	0-1/8	1/8-1/4	1/4-1/2	1/2-1/1
range (V)	0-0.1	0.1-0.2	0.2-0.4	0.4-0.8
ΔX (V)	0.1	0.2	0.4	0.8
dY_{norm} (% of range)	3.12	1.56	0.78	0.39
$PSNR$ (V/V)	32	64	128	256
$SNR(X)$ (V/V)	320X	320X	320X	320X
RDL (%)	2.67	2.67	2.67	2.67
$mean(INL)$ (% of range)	1.33	2	2	2
$INL(X)$ (%)	26.67X	13.33X	6.67X	3.33X

3 Performance evaluation - application

In this section the methodology outlined in section 2 will be applied to four sets of link groups (80 links in total). The links tested differed in terms of the laser transmitter used and the type and number of optical connections. The receiver was of the same type for all tests. One of the link configurations tested was of the same type as distributed to the CMS tracker community for evaluation, consisting of 1310nm lasers, 4-way transmitter and receiver modules, single-mode fibre, and MPO connectors [4].

3.1 Experimental set-up and measurement method

The test arrangement is shown in Fig. 9. The evaluation of the different links is based on the measurement of the system static transfer characteristic [7]. An arbitrary waveform generator (AWG) generates about 100 static voltage levels, X , that are fed sequentially to the laser driver input as a ramp [9]. Synchronization signals for the measuring instruments are also produced by the AWG. For each static measurement point the average, $Y(X)$, and standard deviation, $dY(X)$, of the link output voltage are measured. A high-resolution (12bit) analog to digital

converter (ADC), is used to evaluate the static transfer characteristic and a wide bandwidth (300MHz) oscilloscope is utilized to measure the noise into the system bandwidth. In order to cover the expected system input swing of $\pm 400\text{mV}$, corresponding to an input range of 800mV , an input swing of at least $\pm 500\text{mV}$ is used in all cases. All system outputs are terminated with 50Ω .

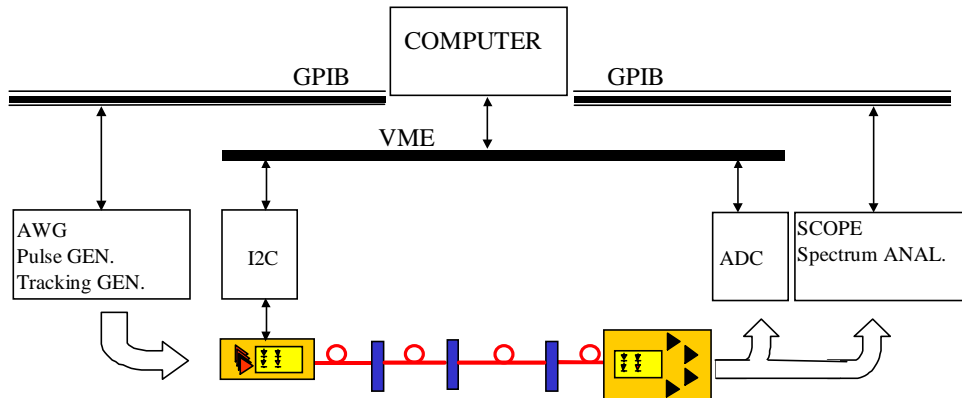


Fig. 9: Test setup for static and noise evaluation.

3.2 Tested link configurations

Four groups of links have been tested as shown in Table 2: Two sets of links with 1-way emitters and two sets of links with 4-way emitters were measured for a total of 80 links.

Table 2: Tested Links

Link	lasertype/manufacture	laser package	# breakpoints	Connector type	# optical channels
A	1310nm, 1-way/X	DIL 1-way	1	FC/PC	20
B	1310nm, 1-way/Y	submount 1-way	1	FC/PC	20
C	1310nm, 1-way/X	DIL 4-way	3	FC/PC	12
D	1310nm, 1-way/X	DIL 4-way	3	MPO	28

The link configuration for the 1-way and 4-way links is shown in Fig. 10 and Fig. 11 respectively. A quad laser driver ASIC supplies current to the laser module. The laser pre-bias is set via an I2C-bus. The laser module pigtail is connected to single-mode patch cords (4-way) or directly to the receiver pigtail. Measurements were performed one channel at a time at $\sim 25^\circ\text{C}$.

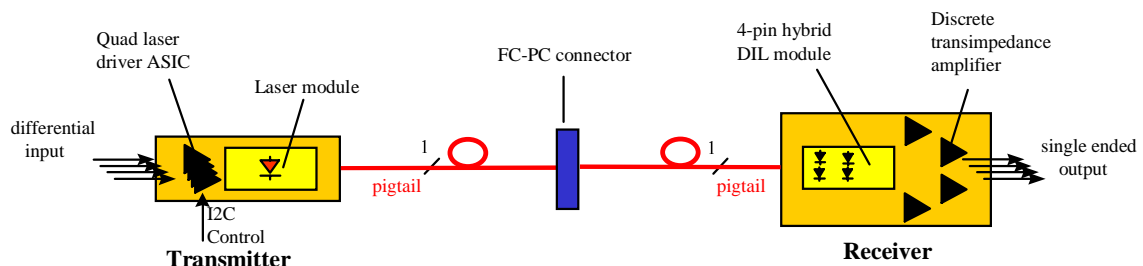


Fig.10: Link configuration for 1-way link test.

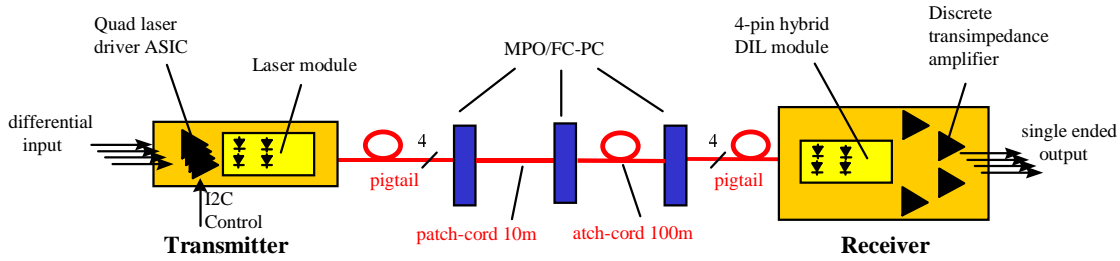


Fig.11: Link configuration for 4-way link test.

It is important to note that the tested links do not exactly conform to the present CMS link baseline [8] as it is foreseen to have links with 1-way emitters, multi-way receivers and three breakpoints using a mixture of 1-way and multi-way connectors. However the measured performance is expected to be close to the final performance of the CMS tracker links. Link D corresponds exactly to the link described in [4].

3.3 Static transfer characteristic

In Fig. 12 the transfer characteristics for link types A, B, C and D are shown. The operating range considered is between 0.0V (thick vertical line) and 0.8V.

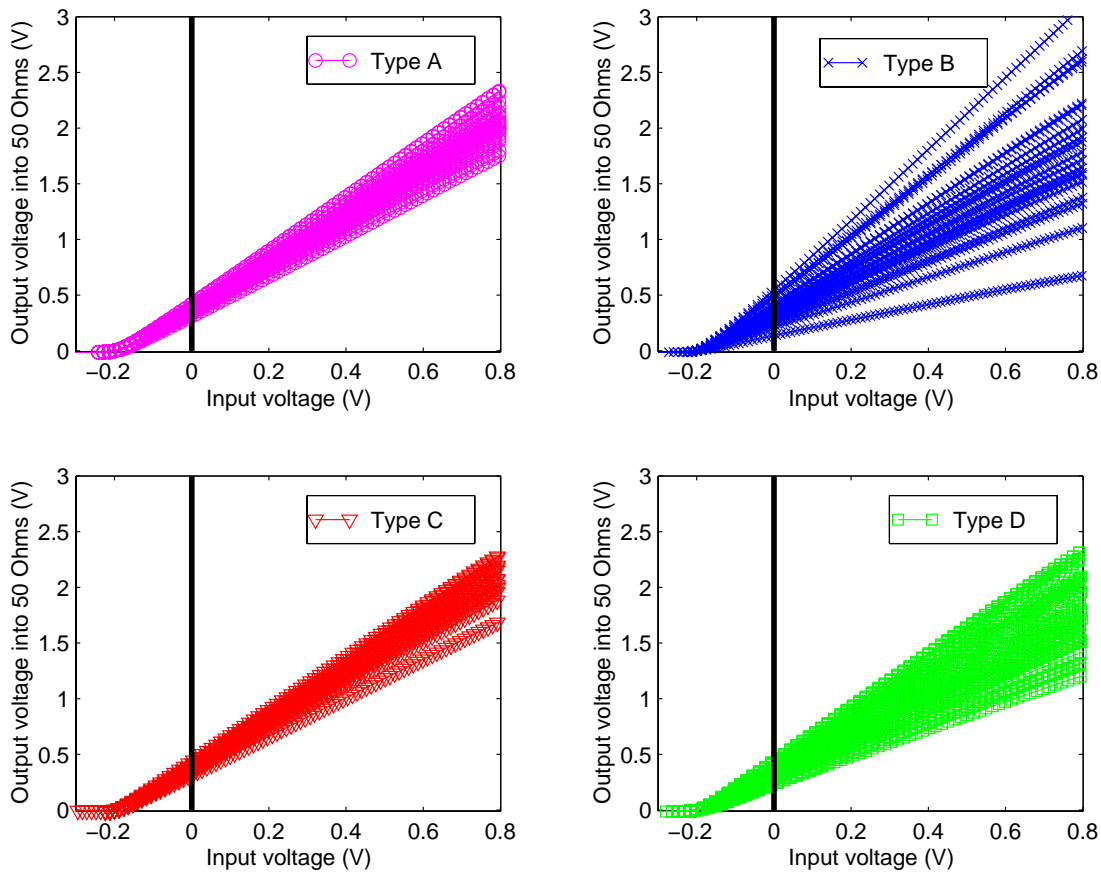


Fig. 12: Measured transfer characteristics for link types A, B, C and D (80 optical channels).

The gains estimated for all links are summarised in Table 3. The average link gain is quite uniform over the four link types at about 2V/V into 50Ω, however the spread around the mean varies between link types, with link type A having the smallest gain standard deviation of 0.16V/V, and link type B the largest at 0.58V/V. A narrow gain

spread is typical of actively aligned laser die, used with a high-quality single-way FC/PC connector (link A and C). A wider gain spread results when a die is passively aligned (link B), or when a multi-way MPO connector is used (link D).

Table 3. Measured link gains

link	gain (V/V)			
	mean	max	min	standard deviation
A	2.1	2.4	1.8	0.16
B	1.9	3.2	0.7	0.58
C	2.1	2.3	1.7	0.17
D	1.9	2.4	1.2	0.34

3.4 Normalised RMS-noise

In Fig. 13 the normalised RMS-noise with $\Delta X=0.8V$ is shown for link types A, B, C and D. Although most of the tested links fall within the specification limit, a few exceed the normalised noise limit by an unacceptable amount. In particular link type B shows excessive normalised noise for input signals above $\sim 0.4V$.

The increase in the normalised RMS-noise with increasing input signals is typical of laser based optical links as the higher optical power induces higher levels of back-reflected light into the laser cavity resulting in more intrinsic laser noise. This particular noise source can usually be controlled either by using angle-cleaved fibre or anti-reflection (AR) coatings at the fibre interface (not used in type B lasers).

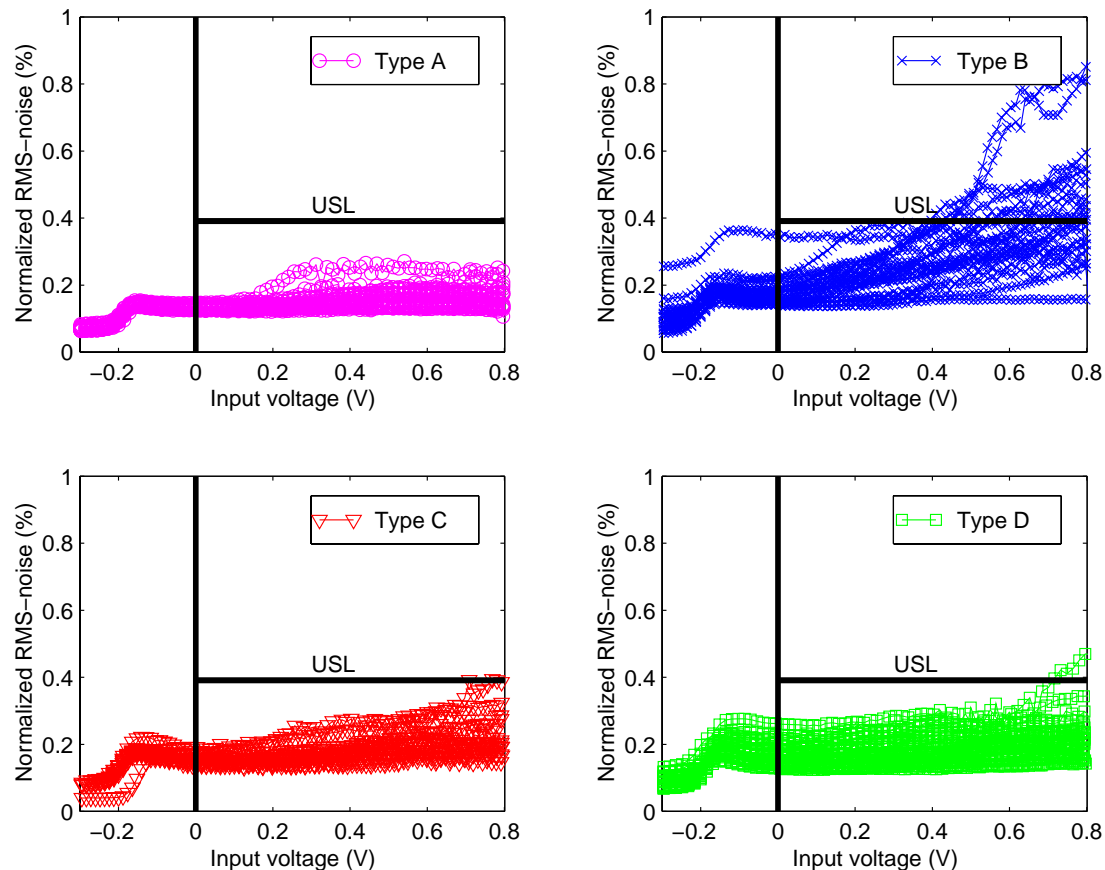


Fig. 13: Normalised RMS-noise for link types A, B, C and D (80 optical channels). Scale on y-axis is in percent of full scale, $G\Delta X$, with $\Delta X=0.8V$.

The average normalised RMS-noise for each of the four regions $k=0, 1, 2, 3$ is shown in Table 4 for each of the four link types tested.

Table 4. Normalised RMS-noise by input range and link type

ΔX (V)	0.1	0.2	0.4	0.8
range	0-1/8	1/8-1/4	1/4-1/2	1/2-1/1
link	average normalised noise (%)			
A	1.0629	0.5398	0.2818	0.1527
B	1.3268	0.7472	0.4403	0.2721
C	1.2442	0.6445	0.3861	0.2004
D	1.2960	0.6568	0.3432	0.1898

3.5 Integral nonlinearity

The integral nonlinearity for link types A, B, C and D is displayed in Fig. 14 for $\Delta X=0.8V$. From Fig. 14 it is clear that linearity is excellent in the fitted region 0.0-0.4V with diverging values at $X>0.4V$. For small signals the linearity diverges due to the proximity of the laser threshold region.

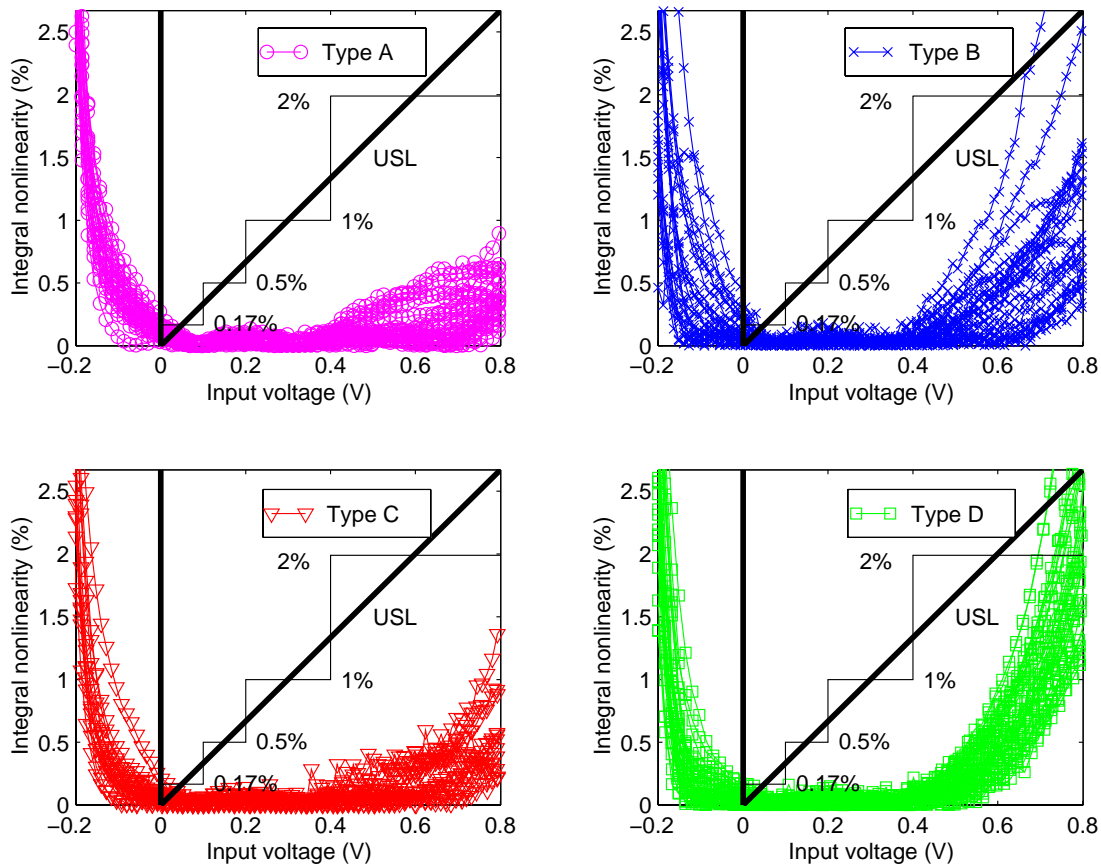


Fig 14: Integral nonlinearity for link types A, B, C and D (80 optical channels).

The average integral nonlinearity for each of the four regions $k=0, 1, 2, 3$ is shown in Table 5 for each of the four link types tested. Scale on y-axis is in percent of full scale, $G\Delta X$, with $\Delta X=0.8V$.

Table 5. Integral nonlinearity by input range and link type

ΔX (V)	0.1	0.2	0.4	0.8
range	0-1/8	1/8-1/4	1/4-1/2	1/2-1/1
link	average integral nonlinearity (%)			
A	0.3275	0.1750	0.0742	0.1644
B	0.3242	0.1542	0.0805	0.3661
C	0.2925	0.1452	0.0807	0.2679
D	0.2595	0.1494	0.0757	0.7287

3.6 Data reduction - averaging of analogue performance measures

3.6.1 Figure of merit for noise and linearity - averaging over input ranges

In Fig. 15 the "Figure-of-merit" plot over 1/2-1/1 of the input range for link types A, B, C and D is displayed. Each measured link is again marked with a symbol for both mean *INL* and *PSNR* with corresponding standard deviations. The specification limits shown are the limit on the peak-signal to noise ratio 256:1 for $k=3$ and the 2% average limit on integral nonlinearity. It is clear that Link type A, C and are within the specification limits for this range. However groups B and C contain a few links with relatively low peak-signal to noise ratio and high *INL*.

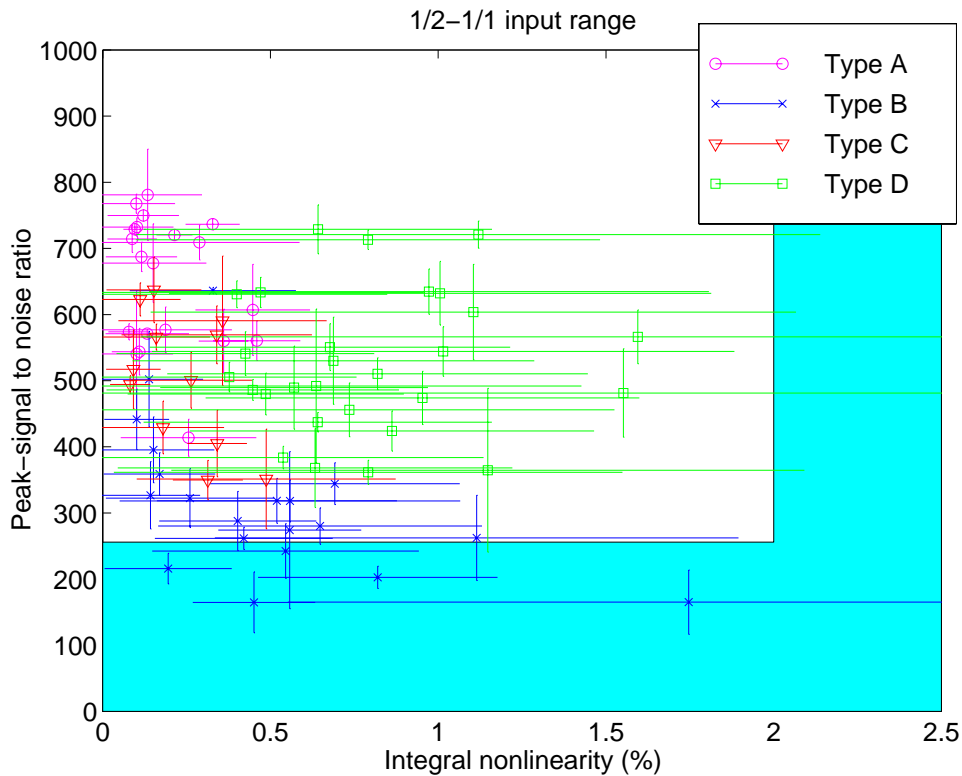


Fig. 15: Figure of merit plot for integral nonlinearity vs. peak-signal to noise ratio for link types A, B, C and D (80 optical channels) over the range 1/2-1/1 of the full input signal of 0.8V. Upper specification limits shown correspond to a signal-to-noise ratio of 256:1 and an integral nonlinearity of 2%.

3.6.2 Figure of merit comparison by group-averages

The final step in the data reduction process is to combine the range-averages with the mean over the number of links in each group. Thus for the peak-signal to noise ratio

$$\overline{\overline{PSNR}}_k = \frac{1}{N} \sum_{i=1}^{i=N} \overline{PSNR}_{ik}, \quad (3-1)$$

where $k=0, 1, 2, 3$. The corresponding standard deviation is

$$\sigma_{PSNR_k} = \sqrt{\frac{1}{N-1} \sum_{i=1}^{i=N} \left(\overline{PSNR}_{ik} - \overline{\overline{PSNR}}_k \right)^2} \quad (3-2)$$

A similar analysis is also carried out for the INL producing

$$\overline{\overline{INL}}_k = \frac{1}{N} \sum_{i=1}^{i=N} \overline{INL}_{ik}, \quad (3-3)$$

with corresponding standard deviation

$$\sigma_{INL_k} = \sqrt{\frac{1}{N-1} \sum_{i=1}^{i=N} \left(\overline{INL}_{ik} - \overline{\overline{INL}}_k \right)^2} \quad (3-4)$$

It is likely that a few spurious bad devices and measurements can significantly affect a set of measurements. Therefore to have a fair estimate of the expected final system performance any data-points that lie beyond 1.5 times the interquartile range (25% to 75% levels around the mean) are considered to be outliers and are consequently not used to evaluate typical system performance. This screening takes place after the data has been averaged over the X -ranges but before the average over devices take place. The result is shown in Fig. 16 for the four ranges, $k=0, 1, 2, 3$. Outliers are marked with symbols without error-bars, and the symbols with error-bars signify the typical behaviour of link types A, B, C and D, in each of the four considered ranges.

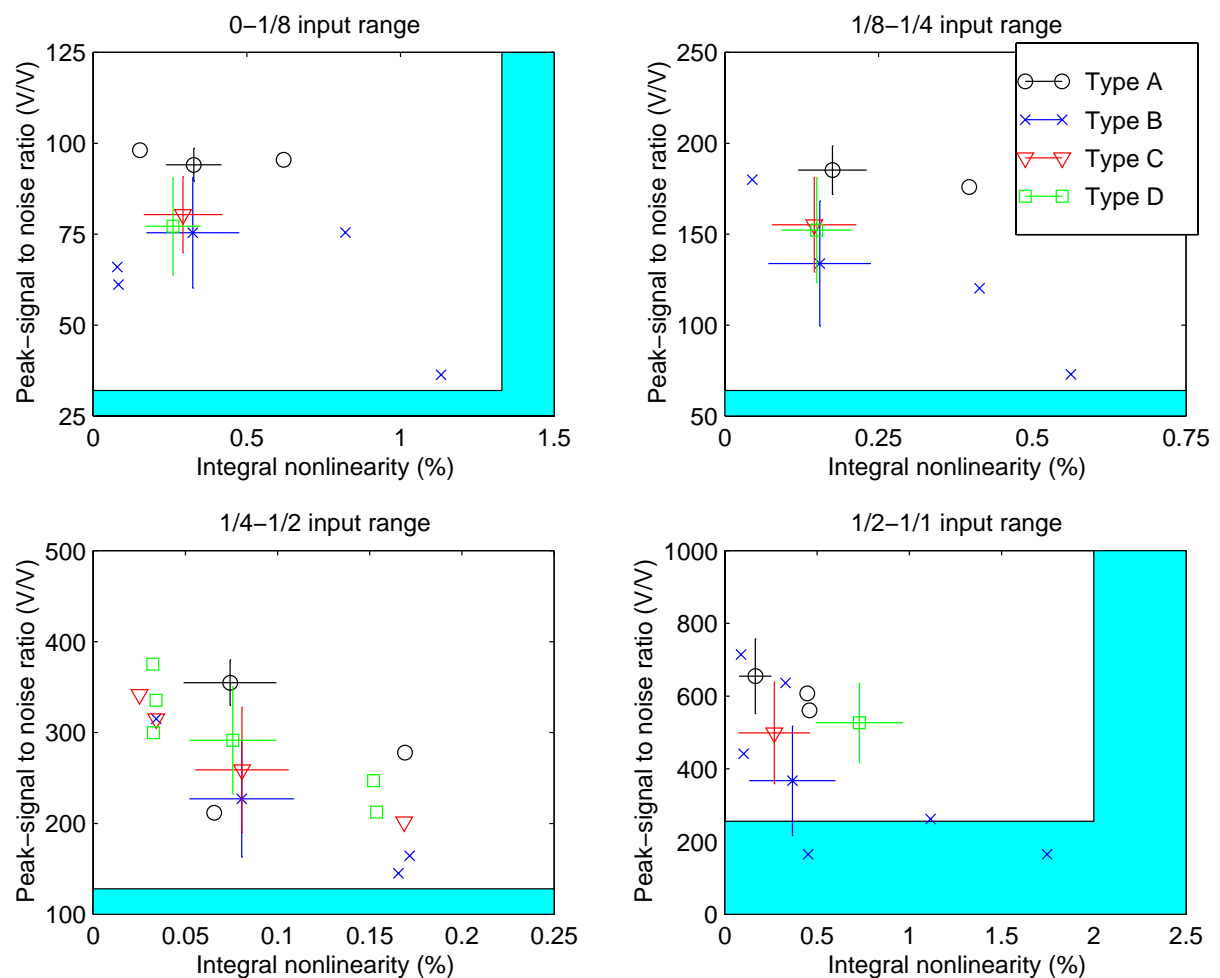


Fig. 16: Peak-signal to noise ratio and integral nonlinearity for range 0-1/8, 1/8-1/4, 1/4-1/2 and 1/4-1/2, averaged over channel number for each link type: A (20 channels), B (20 channels), C (12 channels) and D (28 channels).

After all outliers have been removed it becomes clear that the linearity performance of the four tested link types is quite similar, except in the 1/2-1/1 range where in particular links of type D show higher levels of nonlinearity. Link type A consistently has the highest *PSNR* and type B the lowest in all ranges. The *PSNR* standard deviation of link type B falls below the specification limit in the 1/2-1/1 range, even though 3 *PSNR*-related outliers have been removed. This is clear evidence that there is a problem in this range for type B. However it can be concluded that *typical* system performance is well within the specification limits for link types A, C and D both in terms of linearity and signal-to-noise ratio. It should be remembered however, as the data is range-averaged as well as group averaged, that Fig. 16 might still include atypical links that exceed the specification limits, within limited regions of the input range. The number of outliers is also relatively high, particularly for type B, but this is to be expected in a batch where not all devices are production samples. The existence of a high number of outliers during production however, might indicate device or test problems that should be addressed.

4 Conclusions

A methodology has been developed for analysing the analogue performance of candidate optical links for the CMS tracker read-out system. The method allows typical system behaviour to be extracted and analogue performance to be quantified and compared in an objective way. This is achieved by averaging over parts of the input range, as well as over groups of links, to arrive at a figure-of-merit plot for signal-to-noise ratio and nonlinearity. The described method is also a first step towards a procedure to track performance during the link production and installation phase. During the full-scale production testing of the 50000 optical links for the CMS tracker the described scheme will form the basis for quality control and process analysis, with pass/fail criteria deduced from the specification limits.

Test-data for 80 links of four different types were analysed as an example of how the performance evaluation method can be applied. For each type of link the analogue performance was calculated and compared in figure-of-merit plots. A clear and quantitative ranking could be established in the four operating ranges of interest.

References

- [1] CMS: The Tracker Project. Technical Design Report, CERN/LHCC 98-6, CMS TDR 5, April 1998.
- [2] G.Hall, "Analogue optical data transfer for the CMS tracker, Nuclear Instruments and Methods in Physics" Research A 386 (1997) 138-142.
- [3] F.Vasey, G.Stefanini, and G.Hall, "Laser based optical links for the CMS tracker: options and choices", CMS Note 1997/053.
- [4] F. Vasey et al, "A 4-channel parallel analogue optical link for the CMS-tracker", Proceedings of the fourth workshop on electronics for LHC experiments, Rome, pp. 344-348, 1998,
- [5] K. Gill et. al, "Comparative Study of Radiation Hardness of Optoelectronic Components for the CMS Tracker Optical Links", presented at the RADECS conference, Oxford, Sept. 1998.
- [6] K. Gill et. al. "Ageing test of radiation damaged lasers and photodiodes for the CMS tracker optical links", CMS CR 1999/024.
- [7] G. Cervelli et al., "A Method for the Static Characterisation of the CMS Tracker Analogue Links". CMS Note 1998/043,
- [8] CMS Tracker Optical Readout Link Specification, Part 2: System, Version 3.2, September 1999.
- [9] P. Moreira et. al., "Linear laser driver IC - reference and technical manual", Version 1.0, August 1997.